

# Theoretical Analysis of Length Measurement Using Interference of Multiple Pulse Trains of a Femtosecond Optical Frequency Comb

Dong Wei\*, Satoru Takahashi, Kiyoshi Takamasu, and Hirokazu Matsumoto

Department of Precision Engineering, The University of Tokyo, Bunkyo, Tokyo 113-8656, Japan

Received July 2, 2010; accepted November 8, 2010; published online February 21, 2011

As an alternative to the conventional method of measuring length as a function of the wavelength of a monochromatic laser source, we investigated the possibility of arbitrary distance estimation using the repetition interval of a femtosecond optical frequency comb (FOFC). The investigation is based on an analysis of the formation of the interference fringes of multiple pulse trains. It is found that distance can be measured as a function of the repetition interval between pulses by determining two values from the interference fringes of multiple pulse trains. One is the distance between temporal coherence peaks, and the other is the phase relation between the multiple interference fringes. Theoretical analysis and numerical investigations pave the way for the development of a new length traceability system directly linked to a stable FOFC for both scientific and industrial uses. © 2011 The Japan Society of Applied Physics

## 1. Introduction

In July 2009, the national standard tool for measuring length in Japan changed from an iodine-stabilized helium–neon (He–Ne) laser to a femtosecond optical frequency comb (FOFC). Owing to the outstanding frequency stability of the FOFC (for example, see ref. 1), in the next General Conference of Weights and Measures (Conférence générale des poids et mesures: CGPM), the FOFC is expected as a new standard tool for the International System of Units (SI) of meter. Because the traceability of meter is the infrastructure for both scientific and industrial uses, how to practically perform a distant metrology that is directly linked to an FOFC length standard tool is the most urgent challenge.

The reason for this challenge is that markedly different characteristics exist between a He–Ne laser and an FOFC in both time and frequency domains. In the time domain, a He–Ne laser emits continuous sine wave-shaped light, but an FOFC emits discrete pulse-train-shaped light. In the frequency domain, a He–Ne laser can be simplified as a delta function, but an FOFC can be described as a comb function. Because of these differences, one cannot benefit from the more stable frequency performance of ultraprecision length measurement by just changing the light source from a He–Ne laser to an FOFC in a measurement system (generally, an ordinary Michelson interferometer), which was previously performed by changing the light source from a krypton lamp to a He–Ne laser, since both light sources are used as monochromatic wavelength standard tools.

Previous attempts to solve this problem have not been satisfactory. For example, in 2000, by taking advantage of the frequency domain characteristics of an FOFC, Minoshima and Matsumoto reported on a high-resolution long-distance measurement method used by considering the phase shift of stable intermode beats from the FOFC.<sup>2)</sup> Recently, Yokoyama *et al.* have extended the detection of optical beats to the THz region to perform length measurements.<sup>3)</sup> In the system developed by Minoshima and Matsumoto, a phase meter is required. In the experiment conducted by Yokoyama *et al.*, one needs to synchronize two FOFCs to obtain a stable intermode beat in the THz region. Both systems require more than one FOFC light source.

There are also some studies focusing on the time domain characteristics of an FOFC to challenge this problem. For example, in 2004, Ye proposed a method used by changing the pulse repetition frequency of an FOFC and observing the interference fringes of two pulse trains for a long arbitrary length measurement.<sup>4)</sup> However, because of the trade-off relationship between the stability and variability of the FOFC, it is difficult to achieve both characteristics simultaneously. In 2009, a numerical model of pulse propagation in air was reported by Balling *et al.*<sup>5)</sup> and applied by Cui *et al.*<sup>6)</sup> to length measurements using interference fringes between chirped pulses. However, it is still unknown why different chirped pulses can interfere with each other. If one only considers a single pulse with a Gaussian envelope, the Fourier spectrum of a single chirped pulse in the frequency domain is considered as a Gaussian function. There is no reasonable explanation for the interference phenomenon, because there is no logical indication of the relationship between the two chirped pulses in neither the time nor frequency domain.

As far as the distance-related measurement based on the interference of different pulse trains is concerned, Yasui *et al.*<sup>7)</sup> seem to have been the first to observe the interference of different pulse trains in the 1990s using a femtosecond laser source. In all of these previous works,<sup>4–7)</sup> the observed interference was restricted to only one pair of pulse trains, and few descriptions of the formation of interference fringes were given.

Focusing on these issues, we analyzed the temporal coherence function of an FOFC in our previous work,<sup>8)</sup> and in the present work, we analyzed the formation of interference fringes using the multiple pulse train interference (MPTI) from an FOFC light source. Our results showed that the present multiple pulse train interferometric technique may offer a significantly different possibility to challenge the FOFC directly linked distant metrology problem. For simplicity, we neglected the dispersion and absorption of optical elements over the FOFC illumination bandwidth.

## 2. Principles

For convenience, let us consider the interference fringes formed by a Michelson interferometer with a white light source. Generally, we obtain the intensity of the recombination optical field at the beam splitter as

\*E-mail address: weidong@nanolab.t.u-tokyo.ac.jp

$$I(x, y; k, l) = S(x, y; k)\{a(x, y) + b(x, y)|\gamma[l(x, y)]\cos[(k \times l(x, y))]\}, \quad (1)$$

where  $S(x, y; k)$  is the spectral intensity of the light source,  $a(x, y)$  and  $b(x, y)$  are the spatial intensity distributions resulting from the swings of incident light intensity and heterogeneity of mirror reflectance, respectively,  $k$  is the wave number of the incident light,  $l(x, y)$  is the optical path difference between the points of the measured object and reference mirrors, and  $|\gamma[l(x, y)]|$  is the correlation function at each point of the measured object.

In the case of length measurement using a stable and uniform white light source, eq. (1) can be simplified as

$$I(l) = a + b|\gamma(l)|\cos(k \times l), \quad (2)$$

where  $a = I_{\text{ref}} + I_{\text{obj}}$  and  $b = 2\sqrt{I_{\text{ref}}I_{\text{obj}}}$ ;  $I_{\text{ref}}$  and  $I_{\text{obj}}$  are the intensities reflected by the reference and object mirrors, respectively. Here, we neglect the spatial distribution of the light source used, which is also a controllable parameter for length measurement indicated by Takeda *et al.*<sup>9)</sup> and used by Duan *et al.*<sup>10,11)</sup>

Next, let us determine what will happen in a Michelson interferometer when an FOFC instead of a white light source is used. The correlation function of an FOFC can be expressed as<sup>8)</sup>

$$|\gamma(l)| = F^{-1}[A(f - f_c)] \otimes \sum_{m=-\infty}^{+\infty} \delta(l - m \times c \times T_R), \quad (3)$$

where  $A(f - f_c)$  is the envelope function of the FOFC power spectrum, and  $f_c$  is the center carrier frequency of the FOFC. In the time domain, when the electric field packet repeats at the pulse repetition period  $T_R$ , the ‘‘carrier’’ phase slips by  $\Delta\varphi_{ce}$  to the carrier-envelope phase. In the frequency domain, a mode-locked FOFC generates equidistant frequency comb lines with the pulse repetition frequency  $f_{\text{rep}} = 1/T_R$ . For more details about FOFC time- and frequency-domain descriptions, we recommend refs. 12 and 13. Here,  $F^{-1}$  indicates the inverse Fourier transform, and  $\otimes$  indicates the convolution operation.

If we assume that the FOFC source used shows a Gaussian spectral distribution, we can write

$$|\gamma(l)| = \exp\left[-\left(\frac{2\sqrt{\ln 2}l}{L_{\text{coh}}}\right)^2\right] \otimes \sum_{m=-\infty}^{+\infty} \delta(l - m \times c \times T_R),$$

where  $L_{\text{coh}}$  is the temporal coherence length of one pulse.

When introducing an FOFC with a Gaussian spectral distribution into the Michelson interferometer, we obtain the intensity of the recombination optical field at the beam splitter as

$$I(l) = a + b \times \exp\left[-\left(\frac{2\sqrt{\ln 2}l}{L_{\text{coh}}}\right)^2\right] \otimes \sum_{m=-\infty}^{+\infty} \delta(l - m \times c \times T_R) \times \cos(k \times l). \quad (4)$$

As mentioned above, all of the previous research studies<sup>3-9)</sup> dealt with the single interference fringes, which can be indicated by eq. (4).

Having summarized the steps of the formation of interference fringes between two pulse trains, we now focus on topics that consider the interference fringes formed by

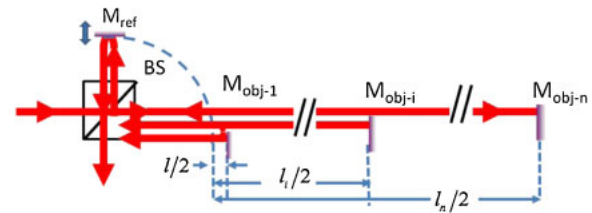


Fig. 1. (Color online) General case of multiple-pulse train interference.

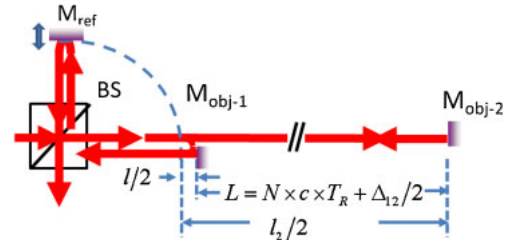


Fig. 2. (Color online) Multiple-pulse train interference for length measurement.

an interference Michelson interferometer of multiple pulse trains, as shown in Fig. 1.

As expressed in eq. (4), different interference fringes occur between different pulse trains. Thus, the total interference fringes are then expressed as the superposition of the MPTI fringes. We obtain the total interference fringes as

$$I(l) = \sum_n I(l_n) = \sum_n \left\{ a_n + b_n \times \exp\left[-\left(\frac{2\sqrt{\ln 2}l_n}{L_{\text{coh}}}\right)^2\right] \otimes \sum_{m=-\infty}^{+\infty} \delta(l_n - m \times c \times T_R) \times \cos(k \times l_n) \right\}. \quad (5)$$

Generally, we cannot further simplify eq. (5). Below, since we discuss the length measurement in this work, we only consider the case  $n = 2$ .

In the case of a monochromatic light source, using the interference, measuring length on the basis of the wavelength of light is a general method. In the case of an FOFC, using the interference, we propose a method of measuring length on the basis of, instead of the wavelength of light, the repetition interval between the pulses from an FOFC as follows.

As shown in Fig. 2, for a given pulse repetition period  $T_R$ , the relationship of the distances between the reference mirror and the two object mirrors,  $l$  and  $l_2$ , and the arbitrary and absolute distance between two object mirrors  $L$  to be measured can be expressed as

$$\begin{aligned} l_2 &= l + L \\ &= l + (c \times T_R)(N + \varepsilon) \\ &= l + N \times c \times T_R + \Delta_{12}, \end{aligned} \quad (6)$$

where  $N$  and  $\varepsilon$  denote an integer ( $N = 1, 2, 3, \dots$ ) and an excess fraction ( $1 \geq \varepsilon \geq 0$ ), respectively. As expressed in eq. (6), to measure the arbitrary and absolute distance  $L$ ,  $N$ , and  $\varepsilon$  should be determined from the MPTI fringes.

As shown below, the integer  $N$  and the excess fraction  $\varepsilon$  can be directly determined by analyzing the resulting temporal MPTI signals, unlike the case of the integer part  $N$  because of the  $2\pi$ -ambiguity of the single-wavelength interferometer.

Note that  $\Delta\varphi_{ce}$  is the phase slippage from pulse to pulse per round-trip length  $c \times T_R$ , and by substituting eq. (6) into eq. (5), we obtain

$$I(l) = a_1 + b_1 \times \exp\left[-\left(\frac{2\sqrt{\ln 2}l}{L_{coh}}\right)^2\right] \times \cos(k \times l) + a_2 + b_2 \times \exp\left[-\left(\frac{2\sqrt{\ln 2}(l + \Delta_{12})}{L_{coh}}\right)^2\right] \times \cos(k \times (l + \Delta_{12}) - N \times \Delta\varphi_{ce}). \quad (7)$$

First, let us investigate the case when the MPTI fringes can be separated.

In the case of  $\Delta_{12} > 2 \times L_{Rey}$  ( $L_{Rey}$  denotes the Rayleigh limit), eq. (7) indicates that by moving the common reference mirror  $M_{ref}$ , we can observe the separated MPTI fringes. Moreover, the distance between the peaks of the separated MPTI fringes  $\Delta_{12}$  and the measured length-related carrier phase slippage of the separated MPTI fringes  $N \times \Delta\varphi_{ce}$  can be presumed from the observed interference fringes. The relationships of the distance between the peaks of interference fringes  $\Delta_{12}$ , the integer  $N$ , and absolute distance between object mirrors  $L$  are expressed as eq. (6). Note that in the frequency domain, the offset shift frequency  $f_{CEO}$  and the pulse repetition frequency  $f_{rep}$  are the only two key parameters used to stabilize an FOFC. The conclusion drawn from the result of the theoretical analysis, that is, an FOFC can be used for not only an extreme-precision frequency metrology but also a high accuracy distant evaluation, is supported by the well-connected time- and frequency-domain expressions  $\Delta\varphi_{ce} = 2\pi f_{CEO}/f_{rep}$  and  $T_R = 1/f_{rep}$ , which can be found in refs. 12 and 13. In other words, with the knowledge of the stable values of  $f_{CEO}$  and  $f_{rep}$  in the frequency domain, we can perform an extreme-precision frequency metrology, as described in ref. 13, and in the time domain, we can perform a high-accuracy distant evaluation by calculating  $N$  and  $\Delta_{12}$  from the separated MPTI fringes.

Owing to restricted equipment availability, we cannot observe the carrier phase slippage  $\Delta\varphi_{ce}$  for the measurement of arbitrary length by stabilizing and changing the offset shift frequency parameter  $f_{CEO}$ . Regarding the separated MPTI fringes, only the measurements of relative distance changes of the interference fringe peaks ( $\Delta_{12}$ ) were carried out in a previous experiment.<sup>14</sup> However, it can be concluded that the feasibility of this proposed method is unquestionable when we consider that the technology of observation and control of the carrier phase slippage has already been established.<sup>15-17</sup>

Next, let us investigate the case when the MPTI fringes overlap ( $\Delta_{12} \leq 2 \times L_{Rey}$ ). By moving the common reference mirror  $M_{ref}$ , we can observe the overlapped MPTI fringes, but we cannot confirm which of these fringes are formed for two mirrors.

From eq. (7), if we assume  $a_1 = a_2$ ,  $b_1 = b_2$ , and  $L = N \times c \times T_R$ , we obtain the total interference fringes as

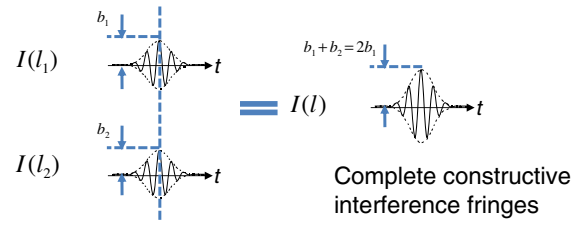


Fig. 3. (Color online) State of complete constructive interference.

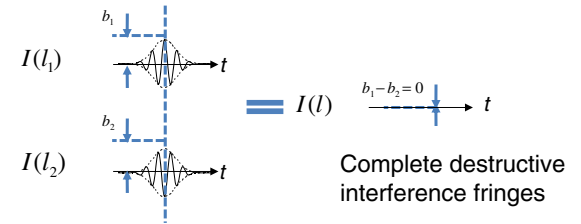


Fig. 4. (Color online) State of complete destructive interference.

$$I(l) = a_1 + b_1 \times \exp\left[-\left(\frac{2\sqrt{\ln 2}l}{L_{coh}}\right)^2\right] \times \cos(k \times l) + a_2 + b_2 \times \exp\left[-\left(\frac{2\sqrt{\ln 2}l}{L_{coh}}\right)^2\right] \times \cos(k \times l - N \times \Delta\varphi_{ce}). \quad (8)$$

By applying

$$\cos(k \times l) + \cos(k \times l - N \times \Delta\varphi_{ce}) = 2 \cos\left(k \times l - N \times \frac{\Delta\varphi_{ce}}{2}\right) \cos\left(N \times \frac{\Delta\varphi_{ce}}{2}\right), \quad (9)$$

we obtain the total interference fringes as

$$I(l) = \begin{cases} 2I_1(l) & N \times \Delta\varphi_{ce} = d \times 2\pi \quad (d = 0, 1, 2, \dots) \\ 0 & N \times \Delta\varphi_{ce} = g \times \pi \quad (g = 1, 3, 5, \dots), \end{cases} \quad (10)$$

where  $I_1(l) = a_1 + b_1 \times \exp[-(2\sqrt{\ln 2}l/L_{coh})^2] \times \cos(k \times l)$  is the conventional white light interference fringe.

One can observe a complete constructive interference (see Fig. 3) and a complete destructive interference (see Fig. 4) between two pairs of pulse trains when the conditions  $N \times \Delta\varphi_{ce} = d \times 2\pi$  ( $d = 0, 1, 2, \dots$ ) and  $N \times \Delta\varphi_{ce} = g \times \pi$  ( $g = 1, 3, 5, \dots$ ) are met. As shown in the numerical examples below, by calculating  $I(l)$  by shifting the parameter  $\Delta_{12}$  in eq. (7), it can be easily observed that the total interference fringes reach an extreme value in both states of the complete constructive and destructive interferences.

After analyzing the formation of the overlapped MPTI fringes, we determine the method of directly linking an FOFC to an absolute length measurement. The basic idea of applying overlapped MPTI to the absolute length measurement is simple. By controlling the carrier-envelope phase of the pairs of pulse trains, one can make the total interference fringes reflected by two mirrors reach an extreme value. When these two interference fringes completely overlap, we obtain only one fixed relation between the two mirrors

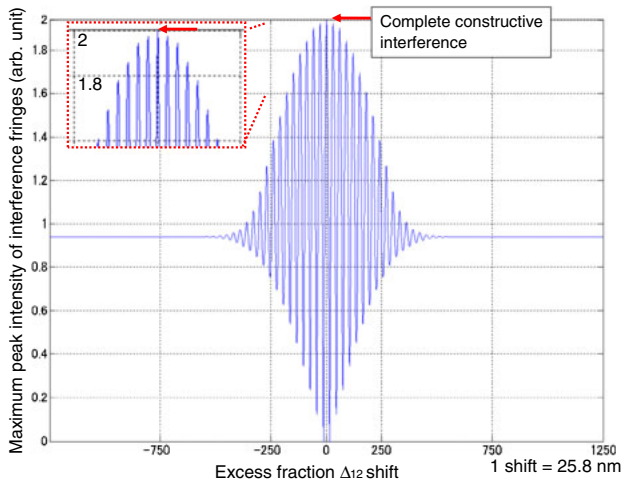


**Fig. 5.** (Color online) Relationship between maximum peak intensity and change in excess fraction  $\Delta_{12}$  [ $N \times \Delta\varphi_{ce} = d \times 2\pi$ , ( $d = 0, 1, 2, \dots$ )].

(as  $L = N \times c \times T_R$ ,  $N \times \Delta\varphi_{ce} = d \times 2\pi$ , or  $N \times \Delta\varphi_{ce} = g \times \pi$ ) and the total interference fringes become minimum or maximum. Conversely, by finding the relatively extreme peaks of the total interference fringes, one can obtain information on the absolute length between two separated points. In a previous initial experiment,<sup>18)</sup> destructive interferences between two pairs of pulse trains were verified.

### 3. Numeral Simulations

To confirm the feasibility of the proposed length measurement method based on the overlapped MPTI fringes, the following simulations are performed. The simulations are carried out with a Gaussian profile and a polarization-mode-locked FOFC. The pulse duration and the repetition rate of the FOFC are 180 fs and 100 MHz, respectively. The output wavelength of the pulse is centered at  $\lambda = 1560$  nm with a spectral width of  $\Delta\lambda = 20$  nm.

In the case of the complete constructive interference, the interference fringes formed for the surfaces of  $M_{ref}$  and  $M_{obj-1}$  are near the interference fringes formed for the surfaces of  $M_{ref}$  and  $M_{obj-2}$ , when the excess fraction  $\Delta_{12}$  between the two mirrors  $M_{obj-1}$  and  $M_{obj-2}$  is reduced. Reduction of the excess fraction  $\Delta_{12}$  means the distance between the mirrors  $M_{obj-1}$  and  $M_{obj-2}$  approaches  $N \times c \times T_R$  in the optical experiment. As noted in Fig. 5, the maximum peak intensity of the acquired interference fringes periodically increases when the excess fraction  $\Delta_{12}$  decreases. When the peaks of two interference fringes completely overlap, by reducing the excess fraction  $\Delta_{12}$  between the two mirrors  $M_{obj-1}$  and  $M_{obj-2}$  to zero, the peak intensity of the acquired interference fringes reach the maximum value of 2 arb. unit.

In the case of the complete destructive interference, as noted in Fig. 6, by reducing the excess fraction  $\Delta_{12}$  between the two mirrors  $M_{obj-1}$  and  $M_{obj-2}$ , the maximum value of the acquired interference fringes is periodically reduced. When the peaks of two interference fringes completely overlap, by reducing the excess fraction  $\Delta_{12}$  between the two mirrors  $M_{obj-1}$  and  $M_{obj-2}$  to zero, the two interference fringes cancel each other out. Thus, the

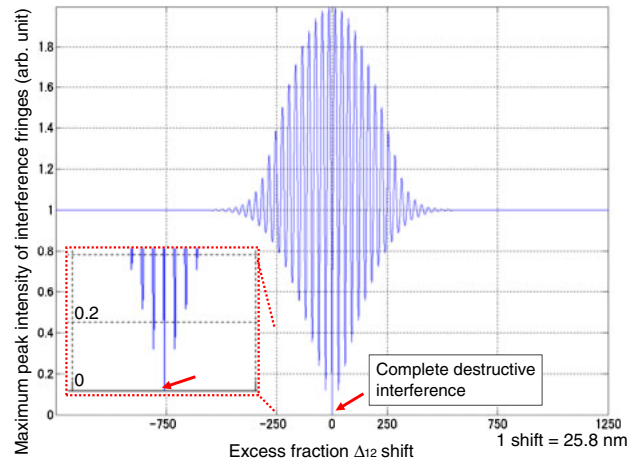


**Fig. 6.** (Color online) Relationship between the maximum peak intensity and change in excess fraction  $\Delta_{12}$  [ $N \times \Delta\varphi_{ce} = g \times \pi$  ( $g = 1, 3, 5, \dots$ )].

peak intensity of the acquired interference fringes becomes 0 arb. unit.

The results of the computer simulation indicate two things. First, there is one-to-one relationship between the relatively extreme peaks of the MPTI fringes and the absolute length between two separated points. Second, it is possible using the data processing method to find the relatively extreme peaks of the MPTI fringes. Unlike the previous experiment reported in ref. 18, this computer simulation shows the mathematical proof and an executable procedure of data processing of the proposed length measurement method.

The conclusion drawn from the results of the computer simulation is that the interferometry of multiple pulse trains can determine absolute distance by employing overlapped MPTI fringes.

### 4. Conclusions

In summary, we have analyzed the formation of interference fringes in a more general case by considering MPTI and expanded the potential application of MPTI. The basic concept is, instead of the wavelength of light, in the case of an FOFC, the repetition interval between adjacent pulses can be used as length reference. To the best of our knowledge, this is the first report that indicates the possibility and shows the detailed proof of measuring absolute distance by observing the interference fringes formatted by MPTI. In the analysis of separated MPTI fringes, the distance between the peaks of the separated interference fringes and the measured length-related carrier phase slippage of the interference fringes, which are linked to the arbitrary and absolute length measurement, can be presumed. In the analysis of overlapped MPTI fringes, the use of the complete constructive and destructive interferences between two pairs of pulse trains for the absolute length measurement has been numerically demonstrated. The results of this investigation show that, with an appropriate optical system, the MPTI can be used as a powerful length measurement tool. Finally, the present concept and analysis pave the way for an MPTI-based metrology.

## Acknowledgments

This research work was financially supported by the Sasakawa Scientific Research Grant from the Japan Science Society (22-216), the “Development of System and Technology for Advanced Measurement and Analysis” Program at the Japan Science and Technology Agency (to H.M.) and the Global Center of Excellence Program on “Global Center of Excellence for Mechanical Systems Innovation” granted to the University of Tokyo, from the Japanese Government. D.W. gratefully acknowledges the scholarships given by Takayama International Education Foundation, Heiwa Nakajima Foundation, and the Ministry of Education, Culture, Sports, Science and Technology of Japan (MEXT).

- 
- 1) Y. Nakajima, H. Inaba, K. Hosaka, K. Minoshima, A. Onae, M. Yasuda, T. Kohno, S. Kawato, T. Kobayashi, T. Katsuyama, and F.-L. Hong: *Opt. Express* **18** (2010) 1667.
  - 2) K. Minoshima and H. Matsumoto: *Appl. Opt.* **39** (2000) 5512.

- 3) S. Yokoyama, T. Yokoyama, Y. Hagihara, T. Araki, and T. Yasui: *Opt. Express* **17** (2009) 17324.
- 4) J. Ye: *Opt. Lett.* **29** (2004) 1153.
- 5) P. Balling, P. Kren, P. Masika, and S. A. van den Berg: *Opt. Express* **17** (2009) 9300.
- 6) M. Cui, M. G. Zeitouny, N. Bhattacharya, S. A. van den Berg, H. P. Urbach, and J. J. M. Braat: *Opt. Lett.* **34** (2009) 1982.
- 7) T. Yasui, K. Minoshima, and H. Matsumoto: *Appl. Opt.* **39** (2000) 65.
- 8) D. Wei, S. Takahashi, K. Takamasu, and H. Matsumoto: *Opt. Express* **17** (2009) 7011.
- 9) M. Takeda, W. Wang, Z. Duan, and Y. Miyamoto: *Opt. Express* **13** (2005) 9629.
- 10) Z. Duan, Y. Miyamoto, and M. Takeda: *Opt. Express* **14** (2006) 655.
- 11) Z. Duan, Y. Miyamoto, and M. Takeda: *Opt. Express* **14** (2006) 12109.
- 12) F. W. Helbing, G. Steinmeyer, and U. Keller: *IEEE J. Quantum Electron.* **9** (2003) 1030.
- 13) J. Ye and S. T. Cundiff: *Femtosecond Optical Frequency Comb: Principle, Operation, and Applications* (Springer, New York, 2005) Chap. 7.
- 14) D. Wei, S. Takahashi, K. Takamasu, and H. Matsumoto: *Jpn. J. Appl. Phys.* **48** (2009) 070211.
- 15) L. Xu, C. Spielmann, A. Poppe, T. Brabec, F. Krausz, and T. W. Hansch: *Opt. Lett.* **21** (1996) 2008.
- 16) S. T. Cundiff: *J. Phys. D* **35** (2002) R43.
- 17) D. J. Jones, T. M. Fortier, and S. T. Cundiff: *J. Opt. Soc. Am. B* **21** (2004) 1098.
- 18) D. Wei, S. Takahashi, K. Takamasu, and H. Matsumoto: *Opt. Lett.* **34** (2009) 2775.